Effects of projected wave climate changes on the sizing and performance of OWCs: a focus on the Atlantic North African and European coastal waters

Irene Simonetti, Lorenzo Cappietti

Abstract—**Reliable estimations of the annual energy production which can be attained with a certain wave energy converter are among the fundamental elements for a sound evaluation of the related levelized cost of energy, which plays a crucial role in the investment decision-making process. The lack of reliability in estimates of the device productivity can, in turn, be a result of the uncertainty in the assessment of the available wave energy resource. The Climate Data Store of the Copernicus Climate Change Service delivers projections of the wave climate along the 20 m bathymetric contours of the whole European coastlines, covering the period 2040-2100, under two Representative Concentration Pathway scenarios (RCP4.5 and RCP8.5). This work addresses the effect of such long-term wave climate changes on the optimal sizing and performances of an Oscillating Water Column wave energy converter to be installed along the North African and European Atlantic coastline. The capture width of the device under different wave conditions is computed using an empirical model capable of predicting the device performance with acceptable accuracy and limited computational time. The results show that the optimal geometry of the OWC varies significantly in the different geographical locations and that the long-term changes in the wave energy resource could cause a slight modification of the optimal geometry in each potential installation site.**

Index Terms—**Oscillating Water Column, Annual Energy Production, Device optimization, Climate change trends, Wave climate trends**

I. Introduction

THE Intergovernmental Panel for Climate Change (IPCC) recognized ocean waves as one of the key climate drivers of coastal hazards in the framework of climate change. The topic of identifying long-term effects of climate change on ocean waves has been recently addressed in several studies, regarding both the identification of trends in hind-cast wave data (e.g. [1], [2] , [3]) and the projection of future waves in a climate change context (e.g. [4]). The robustness and soundness of the projected changes in the wave climate are still under debate. A higher degree of agreement exists on the expected change in mean annual values, while the trend of extreme events has greater uncertainty, with the exception of consistent projections of an increase for the Southern Ocean and a decrease for the North Atlantic area [5], [6]. Recently, Bernardino et al. [7] analyzed the global trends projected up to the end of the 21st century for the mean significant wave height, the wave energy, and the cumulative wave energy, highlighting a significant increase in the South Atlantic, and a decrease of the mean significant wave height and of the average wave energy in the North Atlantic.

The Fifth Assessment Report (AR5) of the IPCC [4] projected climate scenarios induced by different trends in the emissions of Greenhouses Gasses (GHC), defined as Representative Concentration Pathways (RCPs). RCP4.5 and RCP8.5 are, respectively: (i) a scenario with a future radiative forcing of 4.5 $W{\cdot}m^{-2}$, resulting from the hypothesis of the stabilization of GHG emissions before the end of this century, and (ii) a scenario with 8.5 $W{\cdot}m^{-2}$ of radiative forcing, which corresponds to a stable increase of GHG emissions up to 2100. Specifically for the Mediterranean area, studies of the projected wave climate under the RPC8.5 scenario [8] show a decreasing trend of annual mean and maximum values of significant wave height and mean periods over most of the Mediterranean basin. For the same geographical area, Lobeto at al. [4] highlighted a moderate (<1 m) increase in the wave height with a return period of 20 years in the western Mediterranean basin and an opposite decrease in the eastern Mediterranean Sea. In contrast, annual mean values of significant wave height were found to decrease over most of the basin. The divergence of the trend for mean and extreme wave conditions for the Mediterranean basin has been confirmed also in [9], where a general tendency towards more geographically dispersed trends of annual maxima compared to lower percentiles of wave characteristic parameters is observed. Concerning the wave energy resource, significant increasing trends are observed for the mean annual wave power in the Alborean Sea, along most of the western coasts of Italy and the Aegen coasts of Croatia, Grece, and Albania [9]. The studies evaluating the effect of the projected modifications of the wave climate on the power production and on the geometry

The publication was made with the contribution of the researcher I. S. with a research contract co-funded by the European Union - PON Research and Innovation 2014-2020 in accordance with Article 24, paragraph 3a), of Law No. 240 of December 30, 2010, as amended, and Ministerial Decree No. 1062 of August 10, 2021.

I. S. is with the Department of Civil and Environmental Engineering - DICEA - of Florence University, 50139, Florence, Italy (e-mail: irene.simonetti@unifi.it).

L. C. is with the Department of Civil and Environmental Engineering - DICEA - of Florence University, 50139, Florence, Italy (e-mail: lorenzo.cappietti@unifi.it).

Digital Object Identifier:
https://doi.org/10.36688/ewtec-2023-155

optimization of Wave Energy Converters (WEC) are quite limited in the literature. Ulazia et al. ([10], [11]) addressed the issue of the difference in the optimal geometry of an Oscillating Water Column (OWC) device over the four decades between 1979 and 2018 in selected geographical locations along the North-East Atlantic Ocean areas of Europe and Africa. The authors found significant differences between the original device geometry and the geometry optimized including the wave trends. These differences reach a maximum of 15% in some locations, with a variation of up to 20% in the annual average device power production, suggesting the need for a long-term perspective in the sizing and the development of possible control strategies for WECs. A further previous work [9] evaluated the effects induced by long-term wave climate changes, as projected in the RPC8.5 IPCC scenario, on the optimal dimensions and power production of OWC devices along the whole Mediterranean Sea coastline. In this study, relative variations up to 10% in the optimal size of the OWC chamber and applied damping were found, with increases in the annual power production in most of the locations considered.

In this work, we extend the study presented in [9] to consider the effect of long-term changes in the incident wave conditions on OWCs sizing (in terms of chamber size) for the possible installation in different geographical areas, namely the Atlantic coastal waters along Europe and North Africa. The remainder of the paper is structured as follows: the wave data used to characterize the present and future wave climates and the related trends are presented first, followed by the description of the model used to optimize the OWC geometry in each considered location, in the present and in the future wave climate scenario. Results are then presented and discussed.

II. Wave climate projections and trend analysis

The Climate Data Store (CDS) [12] of the Copernicus Climate Change Service provides the time series of hourly wave data for the whole European and North African coastlines (on a 20 m water depth), with a horizontal resolution of 30 km. The dataset includes three climate scenarios: a historical reanalysis based on ERA5 data (for the period 1976-2017), and two projected scenarios corresponding to RCP4.5 and RCP8.5 as defined by the ICPP, covering the period from 2040 to 2100. The CDS dataset contains information on the spectral peak period T_p only, while the spectral period $T_{m-1,0}$ is not provided. For this reason, $T_{m-1,0}$ is determined from the available peak period T_p assuming a theoretical shape of the wave energy spectrum, allowing to obtain

$$T_{m-1,0} = \alpha \cdot T_p \tag{1}$$

For a JONSWAP spectrum with a peak enhancement factor γ=3.3, a value of α=0.904 is obtained. For each grid point on the 20 m bathymetric contours along the whole Atlantic coasts of Europe and North Africa, the available time series of wave data have been analyzed to assess the presence of trends of variation of the available wave power P_{wave}, computed as (2).

$$P_{wave} = \frac{1}{16}\rho \cdot g \cdot H_{m0}^2 \cdot C_g \tag{2}$$

where ρ is the water density, g is gravitational acceleration, and C_g is the wave group velocity obtained by solving the linear dispersion relation on the given water depth h. It is known that (2) provides an approximation of the exact wave power of irregular waves of a given spectrum on finite water depth, but the errors induced by this approximation on the assessment of the wave power assessments, compared to the exact solution, were found to be substantially negligible (i.e., lower than 5%) [13]. The trends in the annual mean value of the wave period $T_{m-1,0}$ are analyzed as well.

The following indexes are used to evaluate the presence of trends in the wave data: (i) the Theil-Sen's slope s [14], which is a non-parametric and robust estimator of the trend in sample data, computed as the median value of all the possible slopes among couples of points; (ii) the p-value of Mann-Kendall tests [15], which indicates to what extent the data are consistent with the null hypothesis (which is, in this case, the absence of long-term trends): for p-values close to 1, data are consistent with the null hypothesis, while p-values close to 0 indicate that the trend in the data is significant.

III. Model of the OWC performance and device optimization

Under the different wave conditions, the energy conversion performance of an OWC is computed by using the empirical Multi-Regression Model (MRM) proposed by Simonetti et al. [16]. The MRM provides the value of Capture Width Ratio CW^* (defined as in Eq. 3) of a rectangular-shaped, fixed, bottom-detached, and asymmetric OWC device (Fig. 1) given the following inputs: wave conditions (H_{m0} and $T_{m-1,0}$), water depth h, geometrical parameters of the OWC (chamber length in the wave propagation direction W, draft of the front wall D and chamber length perpendicular to the wave propagation direction B), and damping applied by the Power Take Off (PTO) system (K). Within the range of its applicability, the model includes the effect of most of the relevant phenomena on the performance of an OWC, including non-linearities, as discussed in depth in [16]. Given the limited computational cost of the model, it is effective for performing optimization studies, where many design alternatives have to be compared.

$$CW^* = \frac{P_{owc}}{P_{wave} \cdot B} \tag{3}$$

In the MRM, the capture width ratio CW^* is be expressed as a function of a set of dimensionless parameters, which were defined based on $\pi - Theorem$, $CW^* = f(h^*, W^*, D^*, K^*)$. The dimensionless parameters are defined as follows:

$$h^* = kh \tag{4}$$

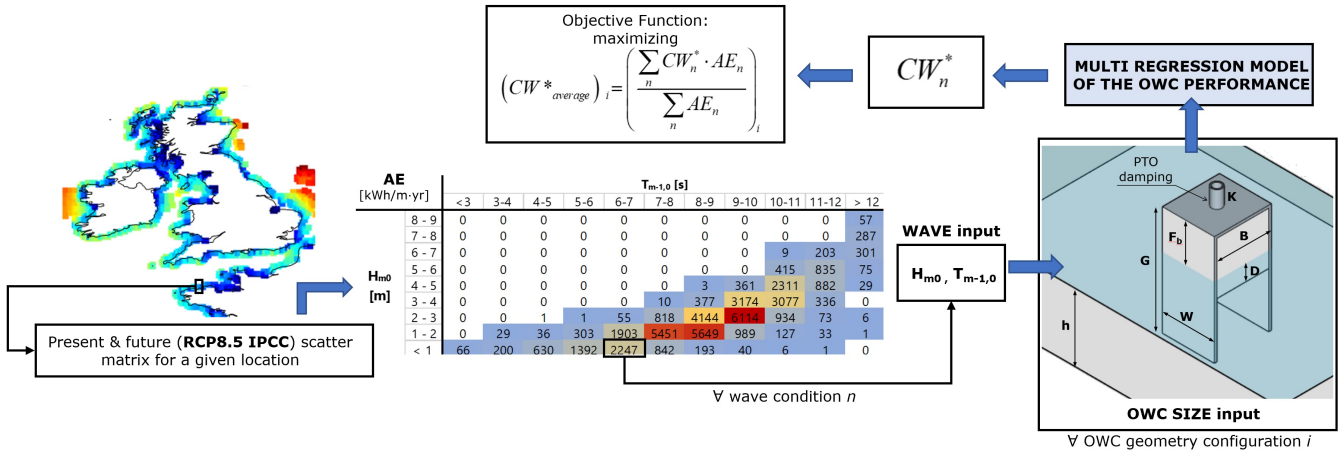

AE [kWh/m·yr] \ $T_{m-1,0}$ [s]	<3	3-4	4-5	5-6	6-7	7-8	8-9	9-10	10-11	11-12	> 12
8 - 9	0	0	0	0	0	0	0	0	0	0	57
7 - 8	0	0	0	0	0	0	0	0	0	0	287
6 - 7	0	0	0	0	0	0	0	0	9	203	301
5 - 6	0	0	0	0	0	0	0	0	415	835	75
4 - 5	0	0	0	0	0	0	3	361	2311	882	29
3 - 4	0	0	0	0	0	10	377	3174	3077	336	0
2 - 3	0	0	1	1	55	818	4144	6114	934	73	6
1 - 2	0	29	36	303	1903	5451	5649	989	127	33	1
< 1	66	200	630	1392	2247	842	193	40	6	1	0

Fig. 1. Methodological approach for the optimization of the OWC dimensions and definition sketch of the design parameters for a fixed, bottom-detached, and asymmetric OWC wave energy converter.

$$D^* = \frac{D}{H \cdot \frac{coshk(h-D))}{cosh(kh)}} \tag{5}$$

$$W^* = \frac{W}{\lambda} \tag{6}$$

$$K^* = K \cdot B \cdot W \cdot \rho_a^{1/2} \tag{7}$$

The functions expressing CW* are the following:

$$CW^* = \frac{f_1(K^* - d(h^*))}{f_2(D^*) \cdot f_3(W^*) \cdot c(h^*)} \tag{8}$$

$$f_2(D^*) = exp(a(h^*) \cdot D^*) \tag{9}$$

$$f_3(W^*) = 1 + (W^* - W^*_{opt})^2 \cdot b(h^*) \tag{10}$$

The reader is referred to the original article [16] for further details on the MRM structure, its derivation, and validation. It is, however, worth stressing that the MRM should be applied only within the range of parameters used for its formulation (i.e.: h^*=1.5–3.5, D^* =1.8–5, W^*=0.08–0.2, K^* =20–170). Moreover, the MRM was specifically formulated for an OWC with the following side ratios of the chamber: $0.67 < B/W < 2$, and values of the ratio of the submerged length of the OWC back wall to the incident wavelength λ which varied between $0.11 < G/\lambda < 0.30$.

In each of the available points on the 20 m bathymetric contours along the whole Atlantic Ocean coastline of North Africa and Europe (from a latitude of 24°N to a latitude of 70°N, i.e. from Western Sahara to Norway), with the resolution in space of 30 km of the CDS data, the MRM is used to evaluate the CW^* of the OWC obtained for different pairs of H_{m0} and $T_{m-1,0}$ pairs, each pair being a cell of the scatter matrix in a specific geographical location. In each location, two different scatter matrixes are comparatively considered: (i) that of the present scenario, obtained based on 30 years of hourly wave data in the CDS database from 1986 to 2016; (ii) the foreseen future scatter matrix, based on projected data from 2071 to 2100 under RCP8.5 emission scenarios (i.e., for the conditions in which the greatest changes are expected compared to the current scenario). All scatter matrixes are discretized in bins of 0.125 m and 0.125 s, for H_{m0} and $T_{m-1,0}$ respectively. In each location and for each alternative scenario, the optimization procedure consists in applying a direct search approach to identify the best-performing geometry: the parameter space to be explored is defined a priori as the set of all possible combinations of W, D and K-values, within a prefixed range and according to a chosen discretization interval. As previously done in [9], we investigated a parameter space composed by values of W between 7 and 11.5 m, D between 3.5 and 6 m (with a discretization interval of 0.2 m), and values of K between 0.6 and 1.5 $kg^{1/2} \cdot$ m$^{-7/2}$ (with an interval of 0.004 $kg^{1/2} \cdot$ m$^{-7/2}$). We assumed constant values of chamber width perpendicular to wave direction (B=10 m), freeboard (Fb=8 m) and length of the lateral al back walls (G=14.5 m). The wave climate of each location has been approximated as a set of regular waves with height $H = H_{m0}/\sqrt{2}$ and period $T_{m-1,0}$, as discussed in [9] and [16]. In each location, for each of the i possible combinations of values of the geometry parameters W, D, K, the Annual Energy Production (AEP) of the OWC is computed as a weighted average of CW^*-values obtained for the n pairs of H_{m0} and $T_{m-1,0}$ of the scatter matrix of the present (or future, in the alternative case) wave climate scenario, as expressed by Eq. 11

$$AEP_i = \frac{\sum_n CW^*_n \cdot AE_n}{\sum_n AE_n} \tag{11}$$

The $i-th$ combination of $(W,\ D,\ K)_i$ associated with the highest AEP is considered as optimal. To account for the decrease in the OWC performance caused by broaching phenomena at the inlet, with the consequent air intake, a reduction factor equal to 0.5 is applied to the predicted CW^* when $H_{m0} > D$. It is recognized that this assumption may cause some inaccuracies in the estimation of the value of CW^*. However, a precise assessment of the decrease of CW^* due to inlet broaching is out of the scope of the present work.

IV. Results

A. Trends in the wave period and in the wave power

As far as the Atlantic Coasts of Western Sahara, Morocco, and Portugal (latitudes between 25°N and 44°N) are concerned, the analysis of the CDS database in the RPC8.5 scenarios (Fig. 2) shows a vast majority of decreasing trends of the average values of wave power P_{wave} (with Theil-Sen's s-values up to -0.025 kW/(m·year) in the South of Morocco and in the Azorean Islands). The p-value of the Mann-Kendall test (Fig. 2, right) suggests that the aforementioned trends are highly significant (i.e. p-value close to 0) in most of the considered areas. Decreasing trends with lower s-values, between -0.005 and -0.01 kW/(m·year), are seen along the North of the coast of Portugal. In this area, Mann-Kendall tests suggest the scarce significance of the trend (p-values are close to 1).

A decreasing trend of the mean annual wave power is foreseen also on the Atlantic coasts of Spain, France, and on most of the Western coasts of the United Kingdom and Ireland for latitudes between 42°N and 62°N and longitudes from -10°W to 5°E (Fig. 3, left). Based on the Mann-Kendall test, such trends are significant, particularly on the West coast of Ireland (Fig. 3, right). The maximum negative s-value associated with this trend is up -0.09 kW/(m·year), i.e. quite remarkable. Decreasing trends, limited in magnitude and scarcely significant, are detected, instead, on the South-East coasts of Ireland and of the United Kingdom (Fig. 3). Opposite increasing trends in the annual average wave power are found in limited areas in the Irish Sea around the Isle of Man, with an s-value up to 0.005 kW/(m·year). Such trends, however, seem to be scarcely significant (with p-values between 0.2 and 0.4).

For further higher latitudes, increasing trends of the annual average value of wave power P_{wave} are observed on the Northern coast of Norway and on most of the Baltic basin (Fig. 4). In this geographical area, the Mann-Kendall test highlights that the trends are significant (with the p-value varying in the range of 0-0.3). Not significant decreasing trends of P_{wave} are observed, instead, in the South of Norway and in the North Baltic Sea area and are limited in magnitude, i.e. s is lower than -0.005 KW/(m·year).

Overall, for the Atlantic coastal waters of Europe and North Africa, the future wave climate projections contained in the CDS under the RCP8.5 scenario seem to be mainly characterized by a decrease of the mean annual wave power. The prevailing decreasing trends of P_{wave} in most of the Atlantic coasts of Europe and North Africa between latitudes of 20°N and 60°N is also confirmed in the recent work of [7]. In the same way, the presence of an increasing trend in P_{wave} for latitudes greater than 65°N, observed in Fig. 4, is also confirmed in [7]. A substantial difference can be highlighted between these results and those obtained for the Mediterranean area by analyzing the same set of projected wave data, where a positive trend (i.e., an increase) of P_{wave}, albeit limited in magnitude, was found for most of the basin [9].

Given the fundamental role of the prevailing wave period in the sizing of the optimal OWC chamber (as discussed, e.g., in [17]–[19]), the trends in the average value of the wave period $T_{m-1,0}$ are also presented. On the Atlantic coasts of Western Sahara, Morocco, and Portugal (Fig. 5), decreasing trends of $T_{m-1,0}$ are found on the whole 20 m bathymetric contour, with s-values varying between -1·10^{-3} s/year and -3·10^{-3} s/year. Such trends are highly significant (Fig. 5, right).

Significant decreasing trends of a similar magnitude are also observed on the Atlantic coasts of Spain, France, and the United Kingdom (Fig. 6), with the most intense decreasing rate (s-value = -3·10^{-3} s/year) localized in the Southern coasts of Ireland and of the United Kingdom. A negligible variation of $T_{m-1,0}$ is expected, instead, along the East coast of Great Britain and Scotland.

For further increasing latitudes, and longitudes between 5°E and 30°E (Fig, 7), the decreasing trend of the mean annual wave period $T_{m-1,0}$ observed for lower latitudes is progressively attenuated, until attaining an opposite increasing trend for latitudes greater than approximately 68°N (Fig, 7, left), on the Northern coast of Norway, where s up to 3.5·10^{-3} s/year. A moderate, but significant, increasing trend in $T_{m-1,0}$ (with $s <$ 0.5·10^{-3} s/year be found also in the Southern Baltic Sea, between Poland and Sweden.

B. OWC device optimization in the different scenarios

As aforementioned, in each geographical location, the MRM of the OWC performance [16] is applied to select the optimal size of the OWC in both the present wave climate scenario (i.e. based on the scatter matrix for 1986-2016) and in the projected wave climate for the period 2071-2100 under RCP8.5 of IPCC. The scatter matrix of each scenario has been discretized with bins of 0.125 m and 0.125 s for the wave height and wave period, respectively. For the application of the MRM, the maximum wave height has been limited to values lower than 5.5 m, considered to be representative of the safe operating conditions for the OWC device and the air turbine. Furthermore, to respect the limits of its applicability, the MRM has only been applied for the wave periods in the range of 4.4 s to 9.2 s.

The value of the OWC chamber draft D influences both its resonance frequency and the dynamic wave pressure acting on the water column. In highly energetic sea states, a reduced value of D may cause inlet broaching, reducing the wave energy conversion capability of the device. The optimal value of D, for each location, results from a balance of these two aspects (as discussed in depth in [9], [17]). On the coasts of Western Sahara and Morocco, as well as in the Canary Islands archipelago, the optimal value of the OWC draft, D_{opt}, varies between 3.5 m and 4 m (Fig. 8,a). In the Azores archipelago, a higher optimal draft is observed (D_{opt}=4-5 m), consistently with a higher relative frequency of wave conditions characterized by greater H_{m0}. D_{opt} values up to 5 m are also obtained in some locations along the Atlantic coast of the Northern Iberian Peninsula. For most of the

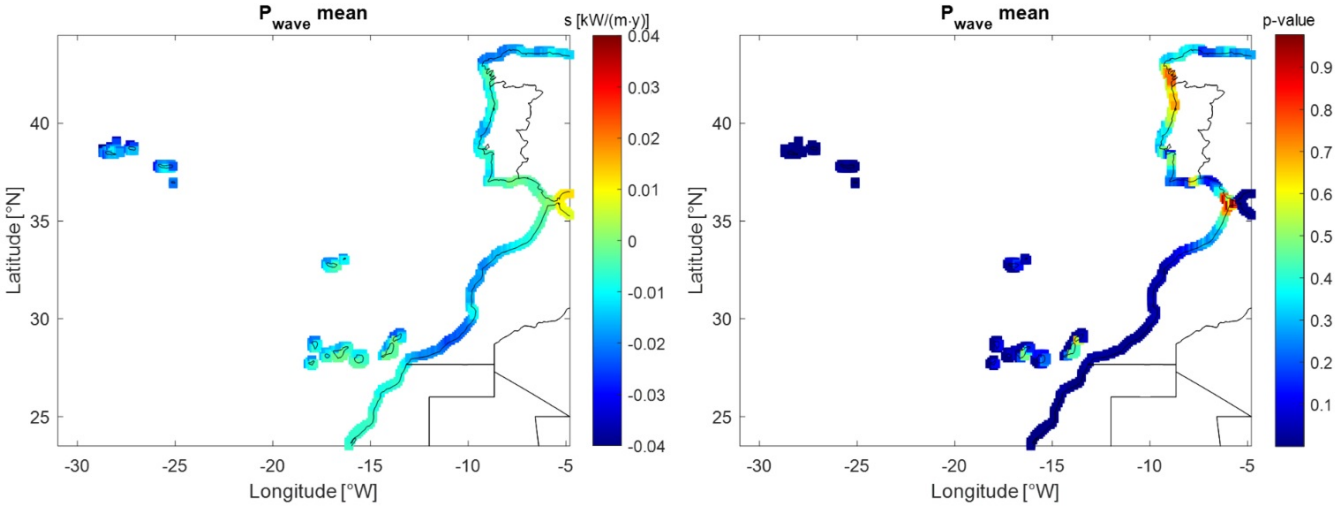

Fig. 2. Spatial distribution of Theil-Sen's slope s (left) and p-value of the Mann-Kendall tests (right) in the IPCC's RCP8.5 scenario on the Atlantic coasts of Western Sahara, Morocco, and Portugal for the annual mean value of specific wave power P_{wave}

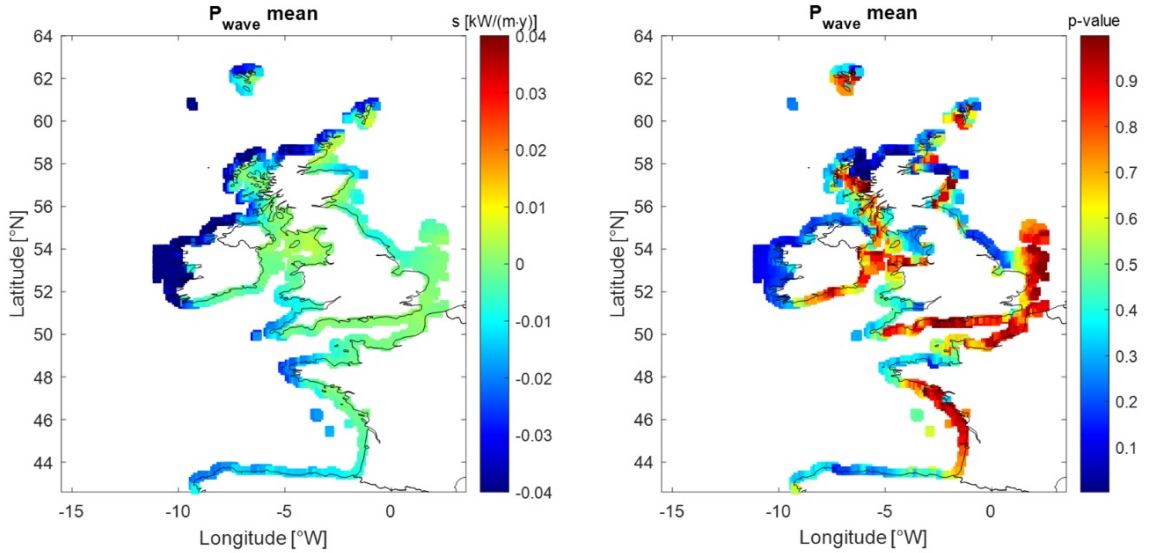

Fig. 3. Spatial distribution of Theil-Sen's slope s (left) and p-value of the Mann-Kendall tests (right) in the IPCC's RCP8.5 scenario on the Atlantic coasts of Spain, France, and the United Kingdom for the annual mean value of specific wave power P_{wave}

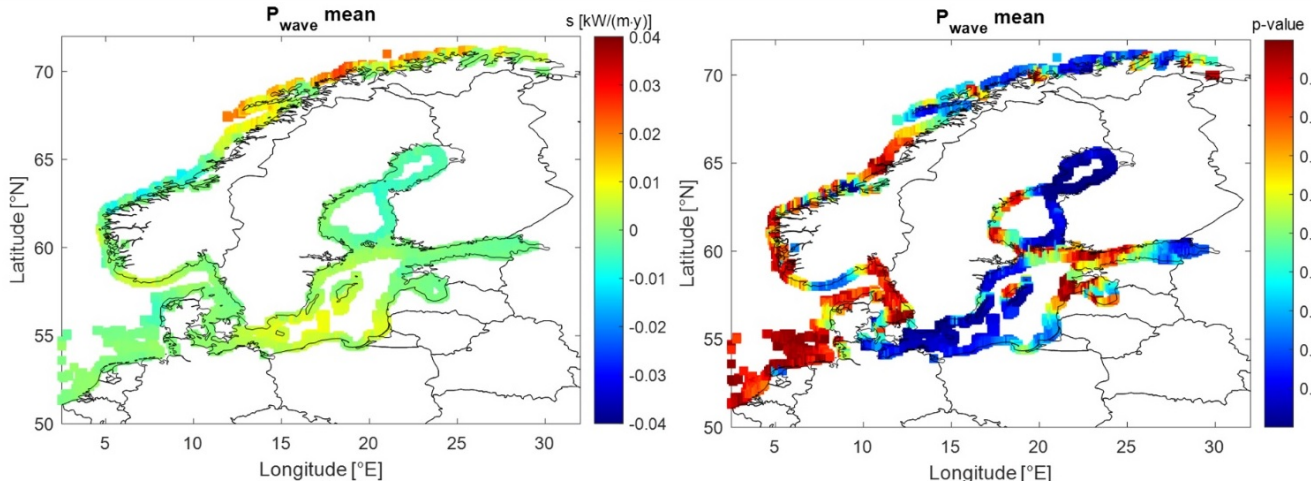

Fig. 4. Spatial distribution of Theil-Sen's slope s (left) and p-value of the Mann-Kendall tests (right) in the IPCC's RCP8.5 scenario along the European coasts of the North, Baltic and Norwegian Seas for the annual mean value of specific wave power P_{wave}

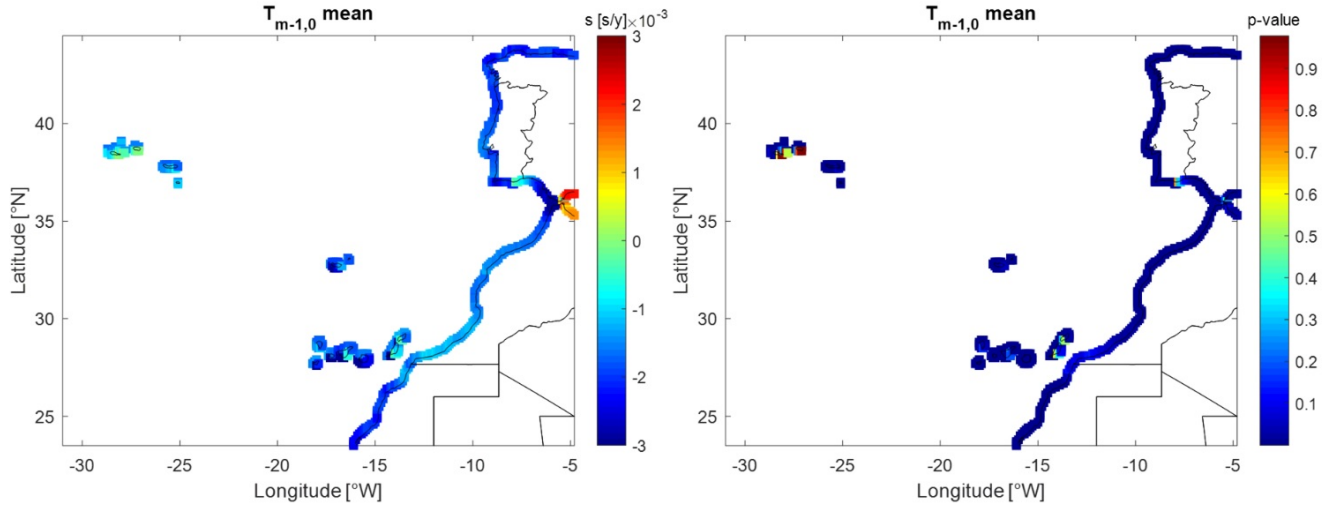

Fig. 5. Spatial distribution of Theil-Sen's slope s (left) and p-value of the Mann-Kendall tests (right) in the IPCC's RCP8.5 scenario on the Atlantic of coasts Western Sahara, Morocco, and Portugal for the mean annual wave period $T_{m-1,0}$

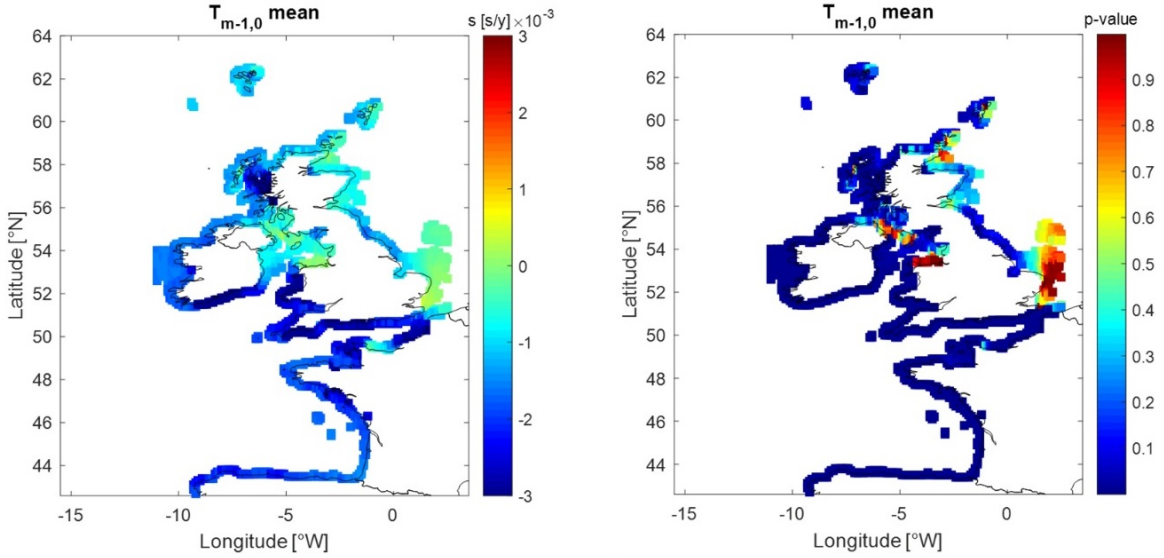

Fig. 6. Spatial distribution of Theil-Sen's slope s (left) and p-value of the Mann-Kendall tests (right) in the IPCC's RCP8.5 scenario on the Atlantic coasts of Spain, France, and the United Kingdom for the mean annual wave period $T_{m-1,0}$

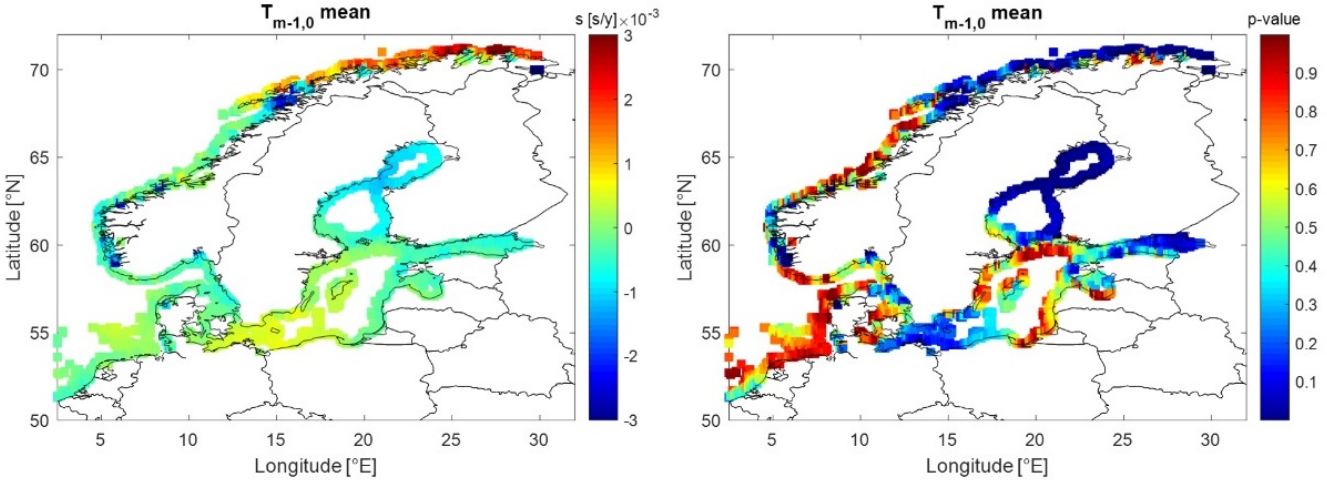

Fig. 7. Spatial distribution of Theil-Sen's slope s (left) and p-value of the Mann-Kendall tests (right) in the IPCC's RCP8.5 scenario along the European coasts of the North, Baltic and Norwegian Seas for the mean annual wave period $T_{m-1,0}$

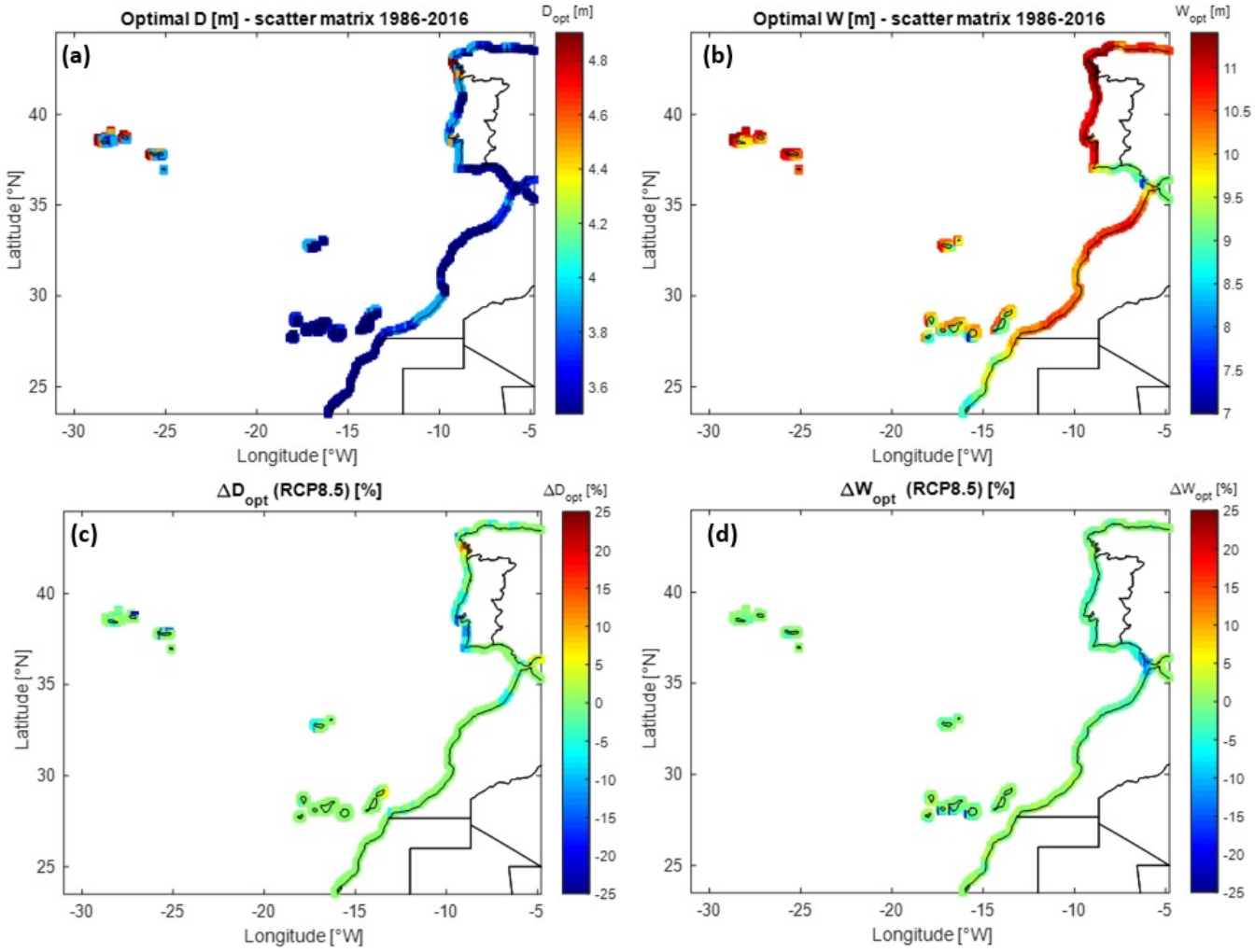

Fig. 8. Optimal values of the OWC chamber draft D (a) and length W (b) obtained for the scatter matrix of the present wave conditions (data from 1986 to 2016) on the Atlantic coasts of Western Sahara, Morocco, and Portugal. Relative variation of the optimal D (c) and W (d) between the present scenario and that projected for the period 2071-2100 under IPCC's RCP8.5 conditions, in the same geographical locations.

locations with latitudes lower than 42°N, the optimal draft of the OWC in the comparative scenario (years 2071-2100, under RCP8.5 of IPCC) shows a limited variation compared to the present scenario (Fig. 8,c). Such variation ΔD_{opt} is of the order of $\pm 5\%$, i.e. it can be considered negligible, except in a limited area in the Northern Iberian Peninsula where ΔD_{opt} attains a maximum of 15%.

The spatial distribution of the optimal OWC chamber length W has been shown to be strongly correlated to the wavelength transporting most of the wave energy in each location [9]. For sites on the 20 m contour lines and latitudes between 25°N and 44°N (Fig. 8,b), the optimal length of the OWC chamber W_{opt} progressively decreases from 11.5 m in the North of the Iberian Peninsula to around 8.5 m along the coasts of Western Sahara. Locally lower W_{opt} values (between 8 and 9.5 m) are found on the Southern coasts of Portugal and Spain. Also regarding the chamber length W, the relative variation of the optimal OWC size from the present wave climate scenario to that projected for 2071-2100 is found to be negligible, being within the range $0 < \Delta W_{opt} < 5\%$ (Fig. 8,d).

For latitudes between 42°N and 64°N and longitudes of -15°W to 5°E (Fig. 9), the optimal OWC draft D_{opt} in the present scenario varies between 3.5 and 4 m along most of the Atlantic coasts of Spain, France, and the United Kingdom, with peaks up to 5.5 m on the Faroe Islands, Shetland Islands and in the West coasts of Central Ireland. Also in this geographical area, the relative variation between the optimal draft in the present and the projected wave climate scenario, ΔD_{opt}, is limited to $\pm 5\%$, with isolated peaks of ΔD_{opt}=15% which are mainly located along the South coast of Ireland (Fig. 9,c). For the same locations, in the present scenario, the optimal OWC length W_{opt} is between 11 and 11.5 m on the Atlantic coasts of Spain, France, along the Western coasts of Ireland and the North of Scotland (Fig. 9,b). Values of W_{opt} around 7 m are obtained in the Irish Sea, due to the limited fetch and the consequent limited value of the prevailing wavelength λ in this area. W_{opt} is between 8 and 9 m in the English Channel area, while it has values of 9.5 to 10 m on the North-East coast of the United Kingdom, in the North Sea. The relative variation of the optimal chamber size is, again, negligible in most locations ($0 < \Delta W_{opt} < 5\%$, Fig. 9,d).

For the latitudes between 52°N and 72°n and longi-

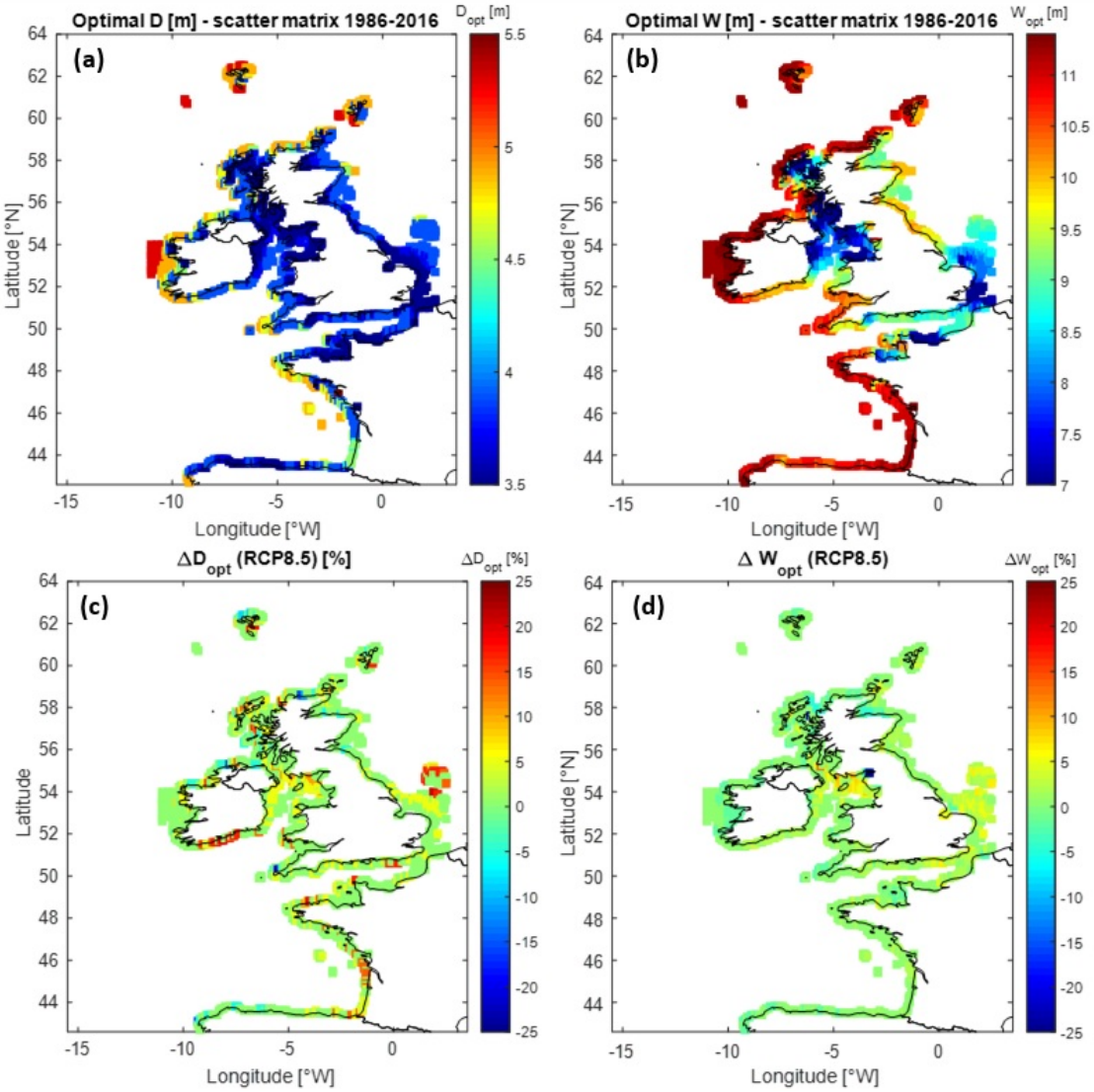

Fig. 9. Optimal values of the OWC chamber draft D (a) and length W (b) obtained for the scatter matrix of the present wave conditions (data from 1986 to 2016) along the European coasts of the North, Baltic, and Norwegian Seas. Relative variation of the optimal D (c) and W (d) between the present scenario and that projected for the period 2071-2100 under IPCC's RCP8.5 conditions, in the same geographical locations.

tudes of 5°E to 30°E (Fig. 10), we find high variability in space of both D_{opt} and W_{opt} along the coast of Norway, with values varying between 3.5 and 5.5 m and 7 and 11.5 m for D and W, respectively (Fig. 10, a and b), and highly scattered. Such a strong variability is a direct consequence of the rugged nature of the Norwegian coast and fjords, with the related variability in the incident wave conditions between sheltered and exposed locations. In most of the Baltic Sea, as in the Finnish Gulf and in the Gulf of Bothnia, the optimal draft D_{opt} is around 3.5 m, while a larger variability is observed for W_{opt}. The optimal OWC geometry under the projected wave conditions for the period 2071-2100 differs negligibly from the present one (Fig. 10, c and d) in the vast majority of the considered locations. Locally higher, but geographically scattered, variations are detected on ΔD_{opt}, with maxima of $\pm 20\%$.

V. Discussion and Conclusion

In this work, an analysis of the possible trends of variation in the future wave climate along the 20 m bathymetric contours in the Atlantic Ocean in front of North Africa and Europe, and on the European coasts of the North, Baltic, and Norwegian Seas is carried out. The data provided by the Climate Data Store of the Copernicus Climate Change Service, which includes projections under the RCP8.5 of IPCC up to 2100, are used. Significant decreasing trends in the annual average wave power are detected for extended areas along the Atlantic coasts of Western Sahara, Morocco, and Portugal and that of Spain, France, and the United Kingdom. Such decreasing trend has the highest magnitude on the West coast of Ireland. A general tendency towards a decrease of the annual average value of the wave period $T_{m-1,0}$ is also found, particularly on the Atlantic coasts for latitudes between 25°N and 60°N. An opposite trend, towards an increase of the annual mean $T_{m-1,0}$, is found in the North of Norway. Focusing on the chamber width and length, this work also analyzes the optimal size of OWC devices to be located on each location along the considered 20 m bathymetric contours, for both

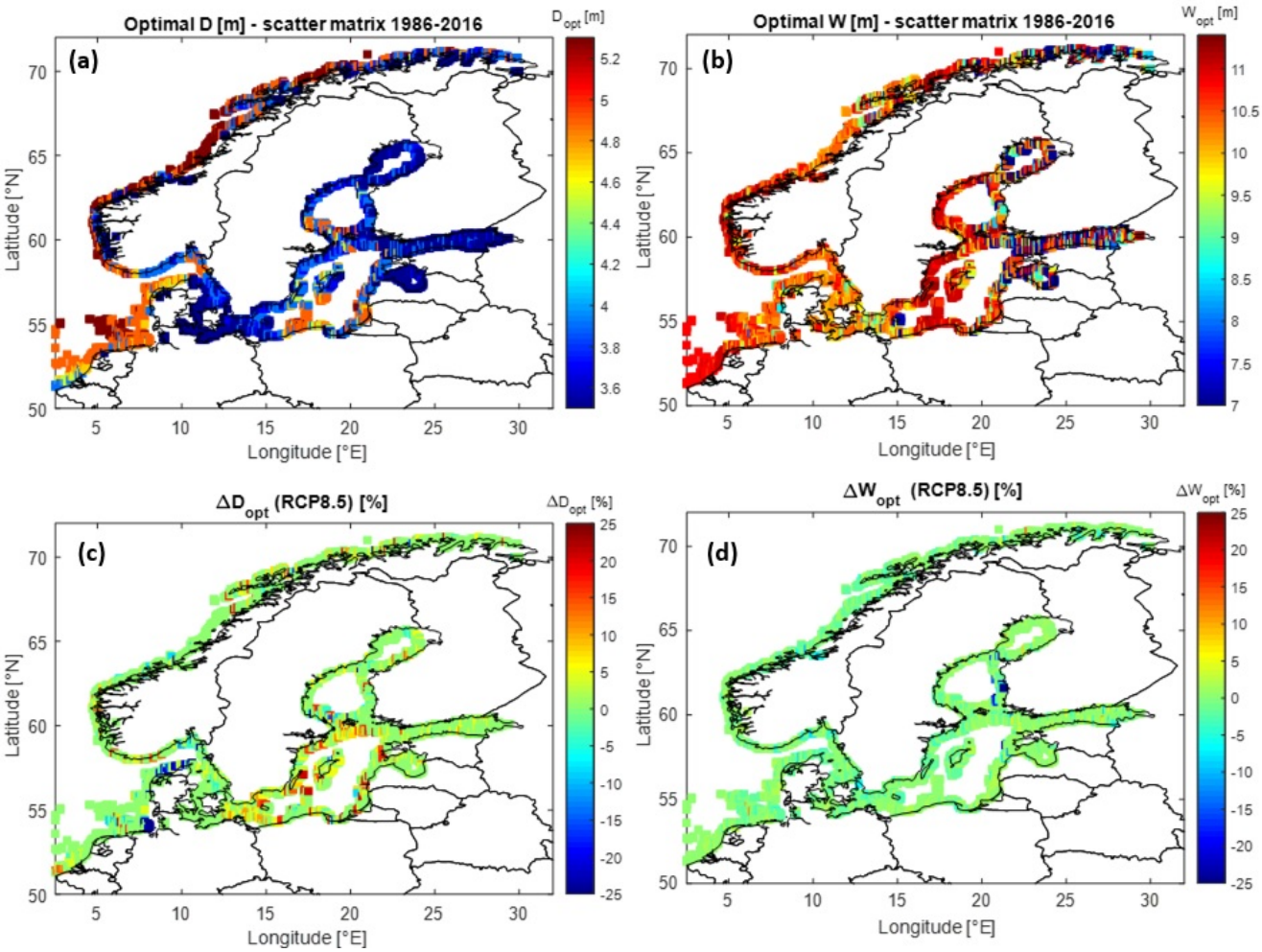

Fig. 10. Optimal values of the OWC chamber draft D (a) and length W (b) obtained for the scatter matrix of the present wave conditions (data from 1986 to 2016) on the Atlantic coasts of Western Sahara, Morocco, and Portugal. Relative variation of the optimal D (c) and W (d) between the present scenario and that projected for the period 2071-2100 under IPCC's RCP8.5 conditions, in the same geographical locations.

the present wave climate and the projected one up to 2100. The regression model developed in [16] is used as a basis to obtain the performance of the device and to carry out the optimization of the geometry. The optimal geometry of the OWC varies significantly among the different geographical locations considered. However, the long-term changes in the wave energy resource seem to cause only slight modifications of the optimal geometry in each potential installation site. Concerning the results obtained in terms of relative variation of the optimal geometry of the OWC, it has to be stressed that the MRM used to calculate the device performance has been formulated with reference to the Mediterranean wave climate, and could only be applied to a limited range of OWC geometries and wave conditions. Therefore, when applying such a model to the Atlantic North African and European coasts and to the Norwegian Sea, where the wave climate is remarkably different from the short fetch conditions which characterize the Mediterranean Sea, the MRM could only be applied on a limited sub-set of wave conditions of each local scatter matrix. For this reason, in the optimization procedure of the OWC geometry in the different locations, only a given fraction of the total available wave energy has been considered as a reference to select the optimal OWC geometry. This may be the reason for the reduced variation in the optimal OWC geometry which is observed when applying the MRM to the projected wave climate for 2100, also in geographical locations characterized by a remarkable trend of variation of the wave power and the characteristic wave period, as the Northern Norwegian coast (as shown in Fig. 4 and in Fig. 7). The effect of such approximations in the accuracy of the results should be further assessed, as a future research work. In the short-fetch areas of the Irish Sea, the North Sea, and the Baltic Seas, a good degree of applicability of the MRM model has been obtained, therefore the results in such areas are affected by lower inaccuracies in the estimation of the optimal OWC geometry and that of the relative change under the projected future wave conditions. In particular, in the Irish Sea, the MRM showed a very high degree of applicability, allowing to carry out the optimization process with reference to couples of H_{m0} and $T_{m-1,0}$ accounting for around 0.9% of the total available wave energy in each location during the procedure of optimization of the geometry (i.e. $\Delta E_{MRM}/\Delta E_{TOT}$=0.9). Also in the North Sea along the eastern coasts of the United Kingdom, the MRM was applicable for a significant frac-

tion of the total wave energy, $\Delta E_{MRM}/\Delta E_{TOT}$=0.7-0.8. The applicability is, instead, reduced to minimum values of $\Delta E_{MRM}/\Delta E_{TOT}$=0.30 in several locations along the Atlantic coasts of Western Sahara, Morocco, and Portugal. Finally, it is worth noting that possible variations of the power performance or of the optimal size of the device induced by variations in the average sea level have not been taken into account in the present work.

ACKNOWLEDGEMENT

This work has been supported by the European Union, FSE-REACT-EU, PON Research and Innovation Programme 2014–2020, D.M. 1062/2021, Contract Number 10-G-15057-1, and is part of the TWIN-COAST research project (https://www.labima.unifi.it/vp-212-twin-coasts.html).

REFERENCES

[1] B. G. Reguero, L. I. J.AU, and F. J. Méndez, "A recent increase in global wave power as a consequence of oceanic warming," *Nature Communications*, vol. 205, pp. 2041–1723, 2019.

[2] I. R. Young, S. Zieger, and A. V. Babanin, "Global trends in wind speed and wave height," *Science*, vol. 332, pp. 451–455, 2011.

[3] A. I. Elshinnawy and J. A. Antolínez, "A changing wave climate in the mediterranean sea during 58-years using uerra-mescan-surfex high-resolution wind fields," *Ocean Engineering*, vol. 271, p. 113689, 2023. [Online]. Available: https://www.sciencedirect.com/science/article/pii/S0029801823000732

[4] H. Lobeto, M. Menendez, and I. J. Losada, "Future behavior of wind wave extremes due to climate change," *Scientific Reports*, vol. 11, p. 7869, 2021.

[5] J. Morim, M. Hemer, N. Cartwright, D. Strauss, and F. Andutta, "On the concordance of 21st century wind-wave climate projections," *Global and Planetary Change*, vol. 167, pp. 160–171, 2018. [Online]. Available: https://www.sciencedirect.com/science/article/pii/S0921818118301073

[6] R. A. Mel, T. Lo Feudo, M. Miceli, S. Sinopoli, and M. Maiolo, "Robustness and uncertainties in global multivariate wind-wave climate projections," *Nature Climate Change*, vol. 9, pp. 711–718, 2019. [Online]. Available: https://www.nature.com/articles/s41558-019-0542-5

[7] M. Bernardino, M. Gonçalves, R. Campos, and C. Guedes Soares, "Extremes and variability of wind and waves across the oceans until the end of the 21st century," *Ocean Engineering*, vol. 275, p. 114081, 2023.

[8] F. De Leo, B. G., and L. Mentaschi, "Trends and variability of ocean waves under rcp8.5 emission scenario in the mediterranean sea," *Ocean Dynamics*, vol. 71, pp. 97–117, 2021.

[9] I. Simonetti and L. Cappietti, "Mediterranean coastal wave-climate long-term trend in climate change scenarios and effects on the optimal sizing of owc wave energy converters," *Coastal Engineering*, vol. 179, p. 104247, 2023. [Online]. Available: https://www.sciencedirect.com/science/article/pii/S0378383922001600

[10] A. Ulazia, A. Saenz-Aguirre, G. Ibarra-Berastegui, J. Sáenz, S. Carreno-Madinabeitia, and G. Esnaola, "Performance variations of wave energy converters due to global long-term wave period change (1900–2010)," *Energy*, vol. 268, p. 126632, 2023. [Online]. Available: https://www.sciencedirect.com/science/article/pii/S0360544223000269

[11] A. Ulazia, G. Esnaola, P. Serras, and M. Penalba, "On the impact of long-term wave trends on the geometry optimisation of oscillating water column wave energy converters," *Energy*, vol. 206, p. 118146, 2020. [Online]. Available: https://www.sciencedirect.com/science/article/pii/S0360544220312536

[12] S. Caires and K. Yan, "Ocean surface wave time series for the european coast from 1976 to 2100 derived from climate projections. copernicus climate change service (c3s) climate data store (cds)," 2020. [Online]. Available: https://cds.climate.copernicus.eu/cdsapp#!/dataset/sis-ocean-wave-timeseries?tab=overview

[13] W. Sheng and H. Li, "A method for energy and resource assessment of waves in finite water depths," *Energies*, vol. 10, no. 4, 2017. [Online]. Available: https://www.mdpi.com/1996-1073/10/4/460

[14] P. K. Sen, "Estimates of the regression coefficient based on kendall's tau," *Journal of the American Statistical Association*, vol. 63, no. 324, pp. 1379–1389, 1968. [Online]. Available: https://www.tandfonline.com/doi/abs/10.1080/01621459.1968.10480934

[15] M. G. Kendall, "A new measure of rank correlation," *Biometrika*, vol. 30, no. 1/2, pp. 81–93, 1938. [Online]. Available: http://www.jstor.org/stable/2332226

[16] I. Simonetti, L. Cappietti, and H. Oumeraci, "An empirical model as a supporting tool to optimize the main design parameters of a stationary oscillating water column wave energy converter," *Applied Energy*, vol. 231, pp. 1205–1215, 2018. [Online]. Available: https://www.sciencedirect.com/science/article/pii/S0306261918314119

[17] I. Simonetti, L. Cappietti, H. Elsafti, and H. Oumeraci, "Optimization of the geometry and the turbine induced damping for fixed detached and asymmetric owc devices: A numerical study," *Energy*, vol. 139, pp. 1197–1209, 2017. [Online]. Available: https://www.sciencedirect.com/science/article/pii/S0360544217314111

[18] M. Hayati, A. H. Nikseresht, and A. T. Haghighi, "Sequential optimization of the geometrical parameters of an owc device based on the specific wave characteristics," *Renewable Energy*, vol. 161, pp. 386–394, 2020. [Online]. Available: https://www.sciencedirect.com/science/article/pii/S0960148120311496

[19] J. Chen, H. Wen, Y. Wang, and G. Wang, "A correlation study of optimal chamber width with the relative front wall draught of onshore owc device," *Energy*, vol. 225, p. 120307, 2021. [Online]. Available: https://www.sciencedirect.com/science/article/pii/S0360544221005569